Measurement of z-direction moisture transport and shrinkage in the drying of paper

WARREN J. BATCHELOR*, ZIQI WU† AND ROBERT E. JOHNSTON‡

SUMMARY

A new experimental rig has been constructed to measure z-directional temperature, moisture and shrinkage during the drying of paperboard. The board to be tested was constructed from three 60 g/m^2 sheets. Shrinkage was measured using eddy current displacement transducers and very thin copper meshes buried between the sheet layers. Moisture content was calculated from the impedance measured between pairs of the copper mesh electrodes. The temperature was measured using very thin thermocouples buried within the sheet. Preliminary measurements on an unbleached eucalypt kraft pulp showed complex drying behaviour, with drying occurring first at the surface in contact with the hot plate and then secondly at the cooler surface where moisture was removed. The middle of the sample was the last to fully dry out. This was in contrast to the shrinkage data, which showed that the bottom layer, from which the water was evaporated, was the last to shrink.

Keywords
Drying, moisture content, impedance, electrical properties, temperature, shrinkage, layers

Paper is formed by impinging a dilute suspension of fibres onto a wire and draining most of the water through the wire, leaving a mat of fibres. After pressing to remove more water the paper is then dried by passing it over a series of steam-heated cylinders. While the forming and pressing sections will have removed more than 99% of the original water, the removal of the remaining amount of water in the dryer section requires the largest amount of energy in the papermaking process. There is great interest in studying the drying of paper so as to maximise the drying efficiency.

* Senior Lecturer,
† Student,
‡ Professor, Australian Pulp and Paper Institute, Department of Chemical Engineering, PO Box 36, Monash University, 3800 Australia.

The process of drying a material with a complicated structure like paper is a very difficult one to model. The basic structure of the sheet is difficult to characterise. The cellulosic fibres from which paper is made are hydrophilic, however, the exact degree will depend on the method by which the fibres have been treated. The fibres will have broad distributions of shapes (length, width, wall area, lumen area) and mechanical properties. Water in paper can be present both as liquid and vapour. Liquid water can be present within the fibres, as free water within the lumens of the fibres, as water droplets between the fibres and adsorbed to the surfaces of the fibres. Both liquid water and water vapour can be transported through the sheet, although the transport of liquid water becomes progressively less important as the sheet becomes dryer (*1*). Various mechanisms for the transport of water and water vapour within the sheet have been proposed, although the importance of each mechanism remains unclear (*2*). Despite the difficulties, there have been numerous attempts to model the drying process (*1*,*3*-*7*). The models have generally been complex, involving a great number of parameters, many of which have not been measured. These models so far have also not considered the shrinkage of the paper during drying, although shrinkage has been included in general models for the drying of hygroscopic materials (*8*). Any successful model will therefore depend heavily on accurate experimental data, in which variables such as shrinkage and moisture profiles are measured.

One of the first papers to make comprehensive measurements of some of these properties was by Han and Ulmanen (*9*). They constructed their test paper by building it up from several thin sheets. They embedded β ray sources between the various layers. By measuring the absorption of the rays as they passed through the sheet, the moisture content of the sheet between source and detector could be determined. In these experiments, the temperature profile was measured by embedding very thin thermocouples between the layers. Shrinkage was only measured for the sheet as a whole and no attempt was made to measure the shrinkage profile in the z (thickness) direction. Drying was studied when their layered sheet of paper was bought into contact with a hot plate. The measured moisture profiles showed a maximum in the middle of the paper. The minimums at the surfaces were caused by the migration of water away from the hot surface and by evaporation into the air from the opposite surface. The measured temperature profiles showed complex behaviour. After initially increasing upon contact with the hot plate, the temperature then remained constant before dipping through a minimum and then increasing. The minimum appeared to be associated with the transition from the so-called constant rate to falling rate periods in drying.

Lee and Hinds (*10*) also reported measurements in which a thick paper pad was bought into contact with a hot surface. They performed their measurements on 600 g/m^2 pads that had been formed from six plies. The temperatures were again measured by fine thermocouples inserted between the plies. No easy way of measuring the local moisture content in the plies was found. Instead, a single drying curve was established through a series of tests. At the end of each test, the sample was pulled from the rig, rapidly delaminated and the moisture content of each layer measured gravimetrically. A complete drying curve was established by varying the moisture content at which the tests were stopped. No attempt to measure shrinkage was made. The convenience of their techniques is severely limited by the need to conduct one test per data point. The reliability of the whole curve is then heavily dependent on the reproducibility of the experimental technique.

During the drying process, moisture moves in the sheet in both liquid and vapour form. Lee and Hinds (*10*) did develop a very interesting technique, using water soluble, non-volatile tracer molecules, to measure the liquid flux in the drying process. After delaminating the sheet to obtain the moisture content in a ply, the sheet was then disintegrated and the tracer molecule concentration measured.

The change in tracer concentration from the previous test point was then used to calculate the liquid flux in the ply. The combined data of moisture content and liquid flux was then used (*1*) to calculate the vapour flux. The results for the vapour flux showed consistent flows away from the hot surface for all of the plies. The measurements of the liquid flux results were more complex, as they showed that liquid water initially flowed into the plies closest to the hot surface. This inflow was ascribed to the need to balance the liquid water vapourised at the hot surface. It was found that, except at the beginning of the drying process when the sheet was still very wet, the flows of liquid water were small compared to the vapour flows.

Kuno et al. (*4*) measured moisture and temperature profiles continuously. Their test material was 300 g/m^2 paper constructed of five 60 g/m^2 sheets. In order to better simulate industrial drying, the paper was dried on a curved element. For the measurement of moisture content they used pairs of electrodes buried between the layers of their paper. The measured impedance between the electrodes was found to be very sensitive to the moisture content of the material between the electrodes. Kuno et al. found that varying the moisture content from 70 to 10% changed the measured impedance by two orders of magnitude. The measured impedance was found to depend on temperature as well as moisture content. Shrinkage of the sheet was not measured.

It was the goal of our research to develop, for the first time, an experimental technique for simultaneously measuring moisture profile, z-direction shrinkage and temperature profile in the drying of paper. This is expected to provide valuable information to aid in understanding this complex process.

MEASUREMENT TECHNIQUES

Our aim was to simultaneously measure moisture content, z-directional shrinkage and temperature at different positions through the thickness of the sheet. The techniques we developed will now be discussed in detail.

Sheet structure

It was decided to make the measurements on multi-layer sheet. While it would be preferable to measure temperature, moisture content and shrinkage continuously through the z-direction of a single layer sheet, no practical means was found to be able to do so. Instead sheets were formed separately and then placed on each other to form the sheet to be tested. This method allowed the thermocouples and electrodes required for the temperature, moisture content and sheet thickness to be placed in appropriate positions. In the work reported here, the sheets were constructed from three 60 g/m^2 handsheets made from a *Eucalyptus globulus* laboratory pulp cooked to a Kappa number of 20. The sheets were made using a British Standard Handsheet machine and pressed at 2 bar using a 'Roll-tech' dynamic press. Some samples were also made at lower grammages so that the effect of sample thickness on the measured impedance could be investigated.

Moisture content

The method chosen for the measurement of moisture content was the impedance method successfully used by Kuno and co-workers (*4,11*). However, the technique was modified by replacing the wire electrodes used by these workers with thin square electrodes. Square electrodes were chosen over wire electrodes to minimise the problems with aligning the electrodes. At a given density and structure the measured impedance may depend on the separation between the wires and hence it becomes critical to ensure that the wires are exactly aligned. These electrodes can also be used as targets for the measurement of displacement (*12*).

In the work reported here, 2 cm x 2 cm square electrodes were chosen. For the full multi-layer drying test, a copper mesh of 25.4 μm thickness was selected for the electrode material. The reasons for this selection are discussed in the section on displacement measurements. Both the leads to the electrode, as well as the electrode itself, were constructed of this mesh. As moisture can penetrate the mesh structure of the electrode, it was expected that the moisture content of the part of the sheet between the mesh electrodes should be the same as in the rest of the ply.

In order to measure the moisture content, the relationship between moisture content and impedance had to be accurately determined. This was done using the calibration rig shown in Figure 1. In the rig, a sample is sandwiched between top and bottom electrodes. The weight applied to the top lid ensured good contact between sample and electrodes. The rig was designed to minimise the escape of moisture from the sample while the sample was under test, which is an important consideration for measurements at high temperature.

To conduct a test, a paper sample was cut to closely fit the test chamber and the electrodes were connected to the LCR meter. The impedance measured in the test was the steady-state impedance. The time to reach a steady state varied with different moisture contents, ranging from a couple of minutes for a very wet sample (>60%) to a few seconds for a relatively dry sample (<15%). After the impedance was measured, the sample was removed and its weight measured with an analytical balance (Mettler Toledo AB204). The moisture content was later calculated from the oven-dry weight of the sample. The measured impedance will depend on the applied weight (*13*). Therefore, the weight on the rig was selected to produce the same compressive stress as would be applied in a full-scale test.

For temperatures higher than 20°C, the whole test unit was put into an oven and preheated to the desired temperature. The sample, which was in a sealed plastic bag to prevent moisture escaping, was also put into the oven to be preheated. After about 15 to 20 minutes the sample was taken out from the bag, put into the test chamber and quickly covered with the test chamber lid. After the impedance reading was taken, the whole test unit was taken out and allowed to cool. The sample was then quickly transferred into a preweighed sealed plastic bag and the actual moisture of the handsheet was determined gravimetrically.

It should be noted that special care had to be taken to successfully obtain the correct data at higher temperatures because the high evaporation rate at these high temperatures can cause significant moisture loss during operation. All the operations had to be carried out quickly to minimise any unnecessary moisture loss in transferring the sample for measurement.

Samples with moisture contents in the range 7 to 60% were tested. Measurements were made at temperatures of 20°C, 30°C, 40°C, 50°C, 60°C, 70°C and 80°C. The dry thickness of each of the handsheets was measured using a Messmer Digi-Cal thickness tester at room temperature.

A typical plot for five handsheet samples of different thickness, at 20°C is shown in Figure 2. The tested samples were 120 to 270 μm thick when dry or 210 to 480 μm thick at 60% moisture content.

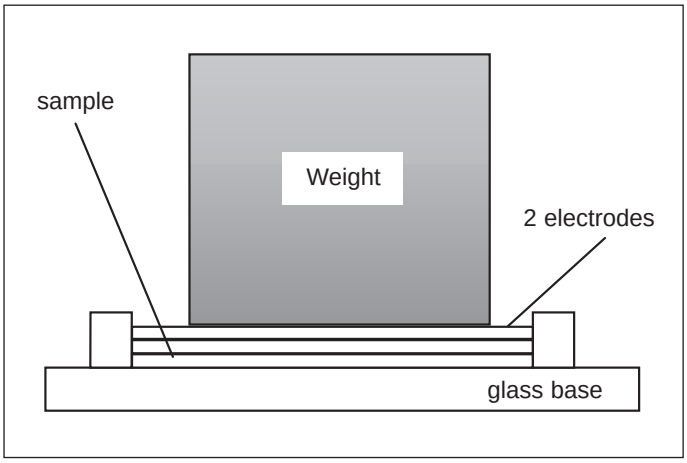

Fig. 1 Experimental rig for calibration of the relationship between impedance and moisture content.

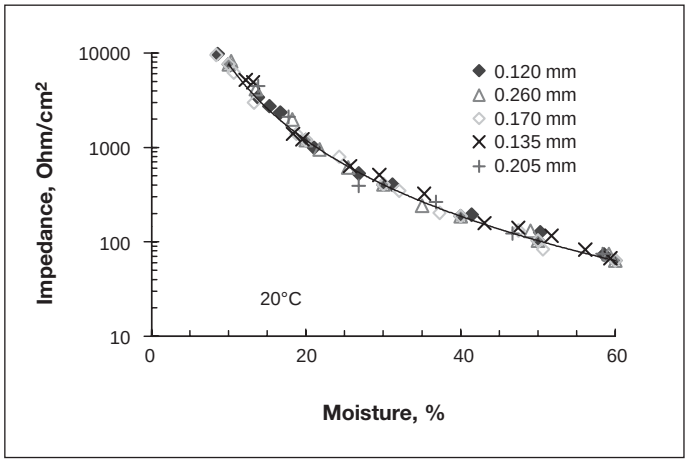

Fig. 2 Impedance vs. moisture content for tests at 20°C.

These values corresponded to a grammage range of 37 to 60 g/m^2. As can be seen from Figure 2, the thickness of tested samples has had no measurable effect on the impedance. This phenomenon was observed at higher temperature, too. The independence of the measured impedance on grammage or thickness was surprising and contrary to expectations. Work is continuing to explain this apparent anomaly.

To obtain an equation for calibration, the data from the tested samples was combined into a single set and fitted using a power law equation. The result of the fit is shown as the line in Figure 2. The R^2 value for the fit (0.99) for the pulp tested indicated that the power law equation provided an accurate representation of the data, giving a simple but relatively accurate method to measure the moisture content.

Besides the tests at 20°C, tests were conducted at 30°C, 40°C, 50°C, 60°C, 70°C and 80°C to study the effect of temperature on impedance. It was found that the impedance generally decreases when the temperature increases, although the effect of temperature on the measured impedance is not nearly as strong as the effect of moisture. The measured decrease in impedance is likely to be due to a fall in the resistance and an increase in the capacitance of the sample. This is because both the resistance and capacitance are largely determined by the mobility of the water molecules and the ions within the sample and the mobility will increase with temperature.

To obtain an equation to describe the effect of temperature, a regression equation was fitted to the experimental results taken at 20 and 70°C. Then a universal equation was derived to predict the impedance at the other temperatures for the moisture content in the range from 10 to 60%. The derived equation is as follows:

$$\begin{aligned} Z &= 10^{x/50} \\ x &= \log\left(1.18x10^5.M^{-1.732}\right) + \\ &(70-T)[\log\left(1.37x10^7.M^{-2.649}\right) \\ &-\log\left(1.18x10^5.M^{-1.732}\right)] \end{aligned} \qquad [1]$$

where Z is the impedance, M is the moisture content, and T is the temperature in °C.

The accuracy of Equation 1 can be seen in Figure 3. This shows the measurements at 50°C. The line shown in this figure was obtained from the calibration equation and was not directly fitted to the data for 50°C. As can be seen in the figure the calibration equation, although not derived from this data set, describes the data very well. The experimental results were found to agree similarly well with the prediction over the complete range of temperature and moisture tested.

The impedance method for measuring moisture content has best accuracy for moisture contents in the range 10 to 50%, which is the range of moisture contents of prime interest in drying studies. Above 50% moisture content, the technique is less accurate because the measured impedances are low and it can be difficult to obtain a stable impedance reading. At moisture contents of 10% or less the slope of the impedance versus moisture content curve begins to increase sharply. Small changes in moisture content produce very large changes in impedance, so small errors in the moisture content measurements will disproportionately affect the accuracy of the data.

Displacement measurements and construction of the full test rig

To measure the shrinkage profile, it was necessary to measure the thickness of each layer. To do this, it was decided to use the copper mesh targets that were already being used for moisture measurements, as eddy current sensor targets. This measurement method works by inducing and detecting eddy currents in metal targets. If the distance between the sensor and target is small then the detected voltage from the sensor will depend linearly on the distance between target and sensor. A copper mesh of 25.4 µm thickness was selected, based on the data of Burton and Sprague (*12*), which showed that for a 25.4 µm thick copper mesh, the deviation of the measurement with the temperature of the target was linear with temperature reaching ~1% at 100°C. A 38.1 µm thick mesh had no deviation with temperature, while for a 12. 7 µm thick mesh, the deviation exponentially increased with temperature reaching 10% at 80°C. The mesh should be as thin as possible to minimise the disruption caused by the presence of the electrode. Accordingly, the 25.4 µm thick mesh was selected as the smallest thickness compatible with a minimal measurement deviation with temperature. As the thickness of the layers varied from 200 µm, when wet, to 100 µm when dry, the mesh has 13 to 25% of the thickness of one of the layers.

The displacement transducers were calibrated for distance by using a micrometer to accurately position the copper target at various distances from the sensor and correlating it against the measured signal. Before each test, the sensors were re-zeroed against the copper mesh targets without the sample. All positions were then measured with reference to this zero position. The thickness of each layer was measured by subtracting the displacement measured for the top of the layer, from the displace-

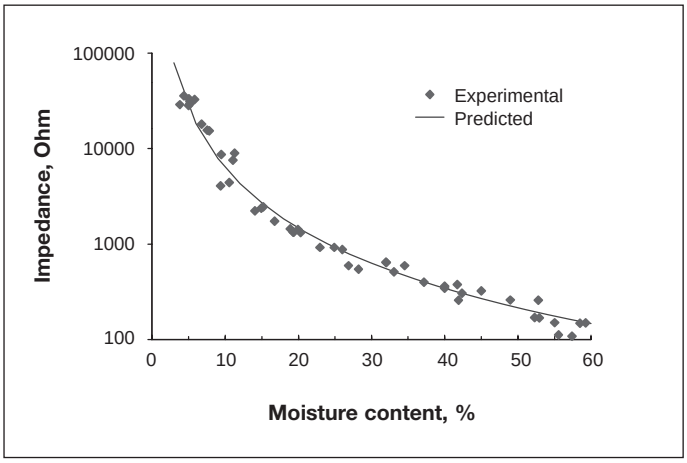

Fig. 3 Comparison between experimental data obtained at 50° and fit predicted from equation 1.

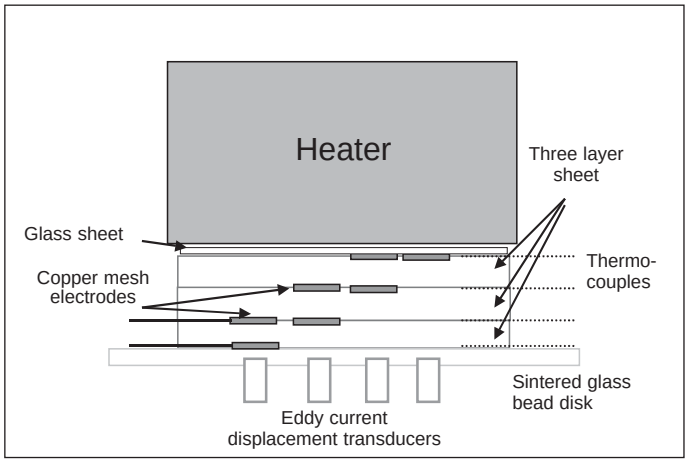

Fig. 4 Schematic of test rig used for full-scale tests.

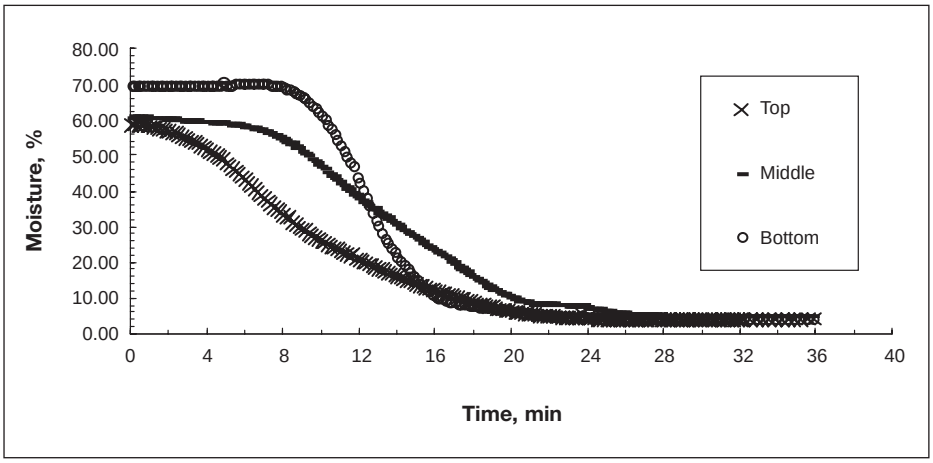

Fig. 5 Measurement of moisture content in the sheet layers during drying.

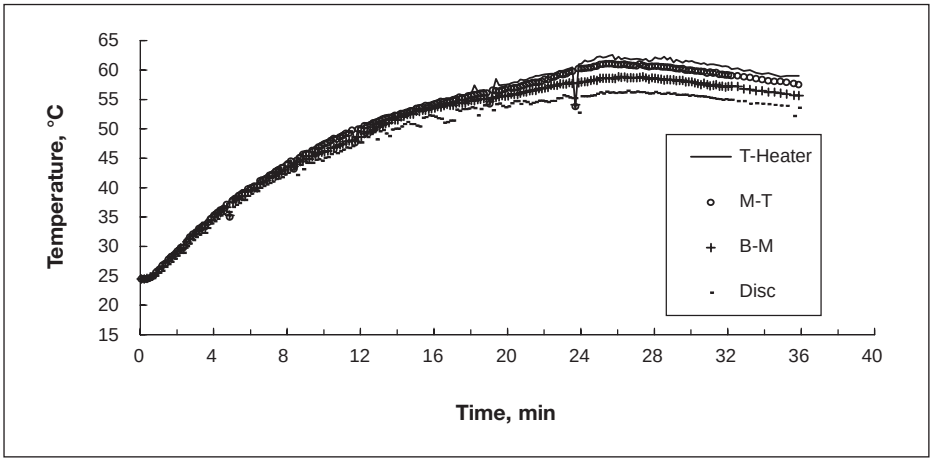

Fig. 6 Measurement of temperature distribution during drying.

ment measured at the bottom of the layer.

The working range of the eddy-current sensors was only 0 to 5 mm and the eddy current sensors were temperature compensated only to 90°C. That is, the displacement readings were assumed to be independent of temperature, provided that the temperature of the sensor was less than 90°C, although for maximum accuracy it was desirable to keep the sensor temperature well under 90°C. Thus it was necessary to find a means of keeping the eddy current sensors separate from the hot paper as well as at the same time supporting the paper and providing a means to remove the evaporated moisture. The other requirements for the supporting material were that it have a low thermal expansion and that it be non-metallic so as not to interfere with the eddy current measurements. The heat source for the experiments was an aluminium block weighing 2.6 kg. A thin glass sheet was placed between the heater block and the sample in order to electrically isolate the heater block from the copper mesh electrodes. The samples themselves were exactly sized to fit under the heater block.

A schematic of the test rig is shown in Figure 4. The key feature to the successful design of the rig is the selection of a sintered disc of fine glass beads for the sample support. This disc plays multiple roles. It supports the weight of the heater block, yet at the same time, the porous nature of the disc allows for the ready transport of moisture away from the paper. The disc also insulates the sensors from the hot paper surface, ensuring that accurate measurements of displacement can be made. The glass bead material was also selected because it has a very low thermal expansion. This ensured that the changes in position of the targets were due to the shrinkage of the sample.

The result is a test rig that allows the moisture content, thickness and temperature of the three layers of the sheet to be measured continuously throughout the test.

RESULTS

A sample set of results is shown in Figures 5 to 7. These figures show temperature, moisture and shrinkage data, respectively.

The moisture data is shown in Figure 5. The initial moisture content of the sample was measured as 60% for two of the plies and 70% for the middle ply. One possible cause for this discrepancy may simply have been that the local moisture content in this ply was higher in the area where the measurements were made. This discrepancy may also be due to the effect

of ageing on the copper mesh electrodes. It was later discovered that problems can arise with the ageing of these copper mesh electrodes, which produces a degree of tarnish on the surface of the electrode. This can significantly affect the measured impedance at very high moisture contents.

The temperature readings are shown in Figure 6. Figure 6 shows four thermocouple readings. The legend indicates the position of the thermocouple. For example, M-T indicates that the thermocouple is placed between the middle and the top layers (closest to the heater) of the sample. Switching the heater block power supply on started the test. Thus the starting temperature of the heater block was room temperature. It is not possible to apply a hot heater block directly to a wet sample, since the impedance measurements take a few minutes to stabilise for a wet sample.

In examining the data, it can be seen that as expected, the thermocouple in direct contact with the heater block has the highest temperature, and that the temperature decreases the farther away the thermocouple is from the heater block. The maximum difference between the thermocouple (marked T-Heater) in contact with the heater block and the thermocouple (marked Disc) is less than 10°C, indicating that there was good thermal contact between the heater block and the top layer and that there was good heat transfer through the layers.

In examining the change in moisture content in the three layers during the test it can be seen that the moisture content in the top layer begins to decrease almost immediately after the heater begins to warm up. This decrease in moisture content is not matched by any change in the thickness of the layer, as is later shown in Figure 7. A possible explanation for the discrepancy could be that as the heater block begins to heat up, evaporation immediately begins to occur at the surface of the sample in contact with the block. The calculated moisture content has a power law dependence on the impedance. Thus while a transfer of moisture from the surface in contact with the heater block to deeper within the layer will not change the overall average moisture content within the layer, it will increase the impedance, due to the disproportionate contribution from the drier layer. Thus, the moisture content data must be treated with caution when there are large moisture gradients.

Despite these reservations, the moisture content data still shows some very interesting trends. As expected the moisture content in the layer closest to the heater (top) begins to decrease first, while the moisture content in the ply furthest from the heater (bottom) starts to decrease from its initial level last. While the top layer always has the lowest moisture content, after 12.5 minutes the moisture content in the bottom layer crosses over that in the middle layer and remains less than that in the middle layer for the remainder of the test. This must be because the moisture transport through the bottom surface into the glass bead disc is exceeding that from the middle ply. The result is a sheet that, in the latter stages of the drying process, has dry surfaces surrounding a wet middle of the sheet.

The shrinkage measurements are shown in Figure 7. The data in this figure show that at the start of the test, the top layer begins to shrink first, followed by the middle layer and then the bottom layer. It is difficult to judge the final thickness of the dry sheet. Over extended periods of time, the measured thicknesses of the layers are not completely constant.

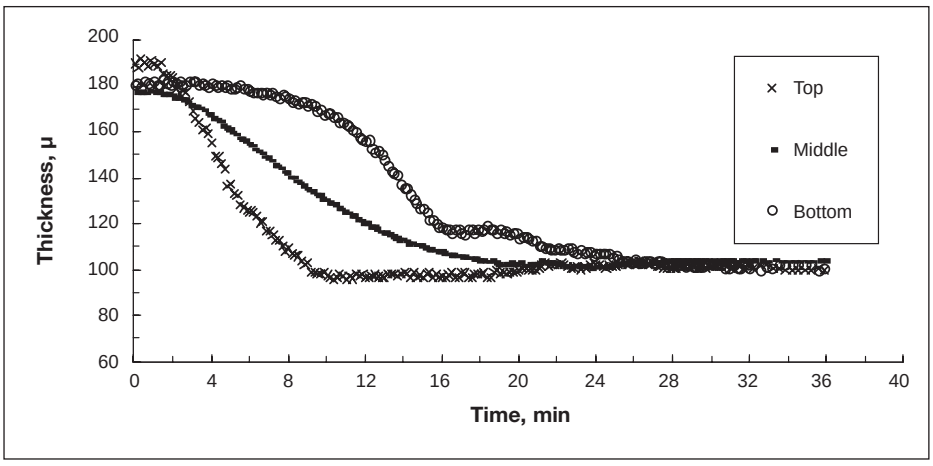

Fig. 7 Measurement of layer shrinkage during drying.

For example, the thickness of the top layer decreases from 190 µm at the start of the test to 97 µm after 8 minutes. Thereafter the measured displacement begins to drift upwards again. The bottom layer appears to shrink continuously for the first 16 minutes of the test. Thereafter the thickness of this layer appears to stabilise for a few minutes before then drifting further downwards. These difficulties with drift may be because each layer thickness is measured by subtracting the displacement measured at the top of the layer from the displacement measured at the bottom of the layer. These displacements are not measured at the same position, which can be a source of error. This will be an increasing problem as the drying test proceeds and the thickness of the layers is reduced. Furthermore for the top layer, the thickness variation at the end of the drying process may also be due to the difference of dryness between top and middle sheets. The dry top sheet will tend to push the target into the wetter middle layer with this process, then reverse once the top layer has fully dried.

The layer thickness data show a somewhat different trend to the moisture content data in Figure 5, since at no point do the thicknesses of the top and bottom layer cross over each other. Except at the start and end of the test, the shrinkage is always greatest in the top layer and least in the bottom layer. The cause of this apparent discrepancy may be that the water is distributed differently between the different phases at different z-direction positions in the sheet. In these drying experiments, the shrinkage of the layers arises from the shrinkage of the fibres, which is in turn controlled by the water content present within the fibre wall. The water in the cell wall in turn is only one component of the total moisture content, which will also include water vapour, free water droplets between the fibres and in the lumen, water adsorbed onto the fibre wall, etc. If the fraction of water distributed between these forms varies with depth in the paper then it is easily conceivable that the relationship between moisture content and shrinkage may be complex. Further work will be conducted to clarify what is happening.

CONCLUSIONS

A new experimental rig has been constructed capable of measuring z-directional temperature, moisture and shrinkage during the drying of paper. Preliminary results on

continued on page 127

Table 1 shows a typical view of the spreadsheet.

An example performance curve is presented in Figure 13.

CONCLUSIONS

The plug flow and the mixed flow methods of modelling a screen have been used to predict thickening across a screen, the concentration profile along the screen, and the screen performance in terms of efficiency of separation. Plug flow behaviour leads to greater thickening than mixed flow behaviour especially at low reject rates, and at the rejects end of the screen. Passage ratio decreases with increasing pulp concentration above a critical concentration, hence the assumption that passage ratio is independent of pulp concentration is not completely valid. Determining passage ratio values from short length screens using the mixed flow model is more accurate than from full-length screens using the plug flow model. Screen performance can potentially be predicted from passage ratio measurements from narrow length screen sections.

ACKNOWLEDGEMENTS

The financial support of the Department of Materials and Process Engineering at the University of Waikato, NZ, is gratefully acknowledged.

REFERENCES

(*1*) Gooding, R.W. and Kerekes, R.J. – Consistency changes caused by pulp screening, *Tappi J.* **75**(11):109 (1992).

(*2*) Gooding, R.W. and Kerekes, R.J. – Derivation of performance equations for solid-solid screens, *Can. J. Chem. Eng.* **67**(5):801 (1989).

(*3*) Kubat, J. and Steenberg, B. – Screening at low particle concentrations, *Svensk Papperstidn.* **58**(9):319 (1955).

(*4*) Steenberg, B. – Principles of screen system design, *Svensk Papperstidn.* **56**(20):771 (1953).

(*5*) Gooding, R.W. and Kerekes, R.J. – The motion of fibres near a screen slot, *J. Pulp Pap. Sci.* **15**(2):J59 (1989).

(*6*) Gooding, R.W. and Kerekes, R.J. – **The passage of fibres through slots in pulp screening,** M.A.Sc. thesis, University of British Columbia, Vancouver, BC, Canada (1986).

(*7*) Kumar, A. – **Passage of fibres through screen apertures,** PhD. thesis, University of British Columbia, Vancouver, BC, Canada (1991).

(*8*) Badger, W.L. and Banchro, J.T. – **Introduction to Chemical Engineering,** McGraw-Hill, New York, p.618 (1955).

(*9*) Weeds, Z. – **The flow behaviour of an industrial screen**, thesis, University of Waikato, Hamilton, NZ (1998).

(*10*) Nelson, G.L. – The screen quotient: a better index for screen performance, *Tappi J.* **64**(5):133 (1981).

Revised manuscript received for publication 2.4.03.

continued from page 111

an unbleached eucalypt kraft pulp showed complex drying behaviour, with drying occurring first at the surface in contact with the hot plate and then secondly at the cool surface where moisture was removed. The middle of the sample was the last part to fully dry out. This was in contrast to the shrinkage data, which showed that the bottom layer, from which the water was evaporated, was the last to shrink.

REFERENCES

(*1*) Lee, P. and Hinds, J.A. – Analysis of heat and mass transfer within a sheet of papermaking fibers during drying, *Proc. 20th Joint ASME/AIChE National Heat Transfer Conference (Paper 81-HT-49)*, ASME, p.1 (1981).

(*2*) Lehtinen, J. – Paper machine drying: A continuing demand for improvements in web properties, runnability and energy usage causes efforts for basic studies, simulation, and experiments, *Proc. 2nd International PIRA conference. Modern Technologies in Pressing and Drying*, PIRA, Paper 13 (1990).

(*3*) Hartley, F.T. and Richards, R.J. – Hot surface drying of paper – the development of a diffusion model, *Tappi J.* **57**(3):157 (1974).

(*4*) Kuno, H., Younosuke, H., Takahashi, Y., and Iwabuchi, M. – Drying mechanism and its numerical simulation in wet and porous media, *Oji Seminar on Advanced Heat Transfer in Manufacturing and Processing of New Materials*, p.PM2 (1990).

(*5*) Ramaswamy, S. and Holm, R.A. – Analysis of heat and mass transfer during drying of paper/board, In Mujumdar, A.S. (ed.) **Drying '92**, Elsevier Science Publishers, p.973 (1992).

(*6*) Ramaswamy, S. and Holm, R.A. – Analysis of heat and mass transfer during drying of paper/board, *Drying Technology* **17**(1-2):49 (1999).

(*7*) Reardon, S.A., Davis, M.R. and Doe, P.E. – Computational modeling of paper drying machines, *TAPPI J.* **83**:58 (2000).

(*8*) Hawlader, M.N.A., Ho, J.C. and Qing, Z. – A mathematical model for drying of shrinking materials, *Drying Technology* **17**(1&2):27 (1999).

(*9*) Han, S.T. and Ulmanen, T. – Heat transfer in hot-surface drying, *Tappi J.* **41**(4):185 (1958).

(*10*) Lee, P. and Hinds, J. - Measurements of heat and mass transport within a sheet of papermaking fibres during drying, *Drying '80 Proceedings of the Second International Symposium*, Hemisphere Publishing Corp, p.523 (1980).

(*11*) Hoshi, Y., Kuno, H., Hashimoto, R., Iwabuchi, M., Yanagi, K. and Yoshida, S. – Simultaneous measurements of temperature and moisture content profiles of paper in drying process, *Nippon Kikai Gakkai Ronbunshu, B Hen* **63**:1035 (1997).

(*12*) Burton, S.W. and Sprague, C.H. – Instantaneous measurement of density profile development during web consolidation, *J. Pulp Pap. Sci*. **13**:145 (1987).

(*13*) Wu, Z.Q., Batchelor, W.J. and Johnston, R.E. – Development of an impedance method to measure the moisture content of a wet paper web, *Appita J.* **52**(6):425 (1999).

Revised manuscript received for publication 1.4.03.